

# On the Thermal Gelling of Ethyl(hydroxyethyl)cellulose and Sodium Dodecyl Sulfate. Phase Behavior and Temperature Scanning Calorimetric Response

Geng Wang,<sup>†</sup> Katarina Lindell,<sup>‡</sup> and Gerd Olofsson<sup>\*,†</sup>

*Divisions of Thermochemistry and Food Technology, Chemical Center, University of Lund, P.O. Box 124, S-221 00 Lund, Sweden*

*Received January 26, 1996; Revised Manuscript Received June 20, 1996<sup>®</sup>*

**ABSTRACT:** High-sensitivity differential scanning calorimetry (HSDSC) experiments and phase studies have been combined in order to investigate thermal events, possibly related to thermoreversible gelation, in semidilute aqueous systems of ethyl(hydroxyethyl)cellulose (EHEC) and sodium dodecyl sulfate (SDS) in the temperature range 20–80 °C. The phase behavior of two gelling EHEC samples in 0.50 and 1.00 wt % aqueous solution containing varying amounts of SDS has been characterized. Both samples formed thermoreversible gels in 1.00% solutions at SDS concentrations above 2 mmol kg<sup>-1</sup>, while in 0.50 wt % solution only one sample formed a gel and now in a restricted region of temperature and SDS concentration. Large, well-defined endothermic peaks were seen in DSC traces of the gelling EHEC samples in pure water. The peaks appeared at about the clouding temperature (CP) of the solutions. Surfactant-free solution of a more hydrophilic (nongelling) EHEC only gave a small heat capacity shift at CP. The transition peaks observed for the gelling EHEC in pure water are considered to indicate that polymer association through interaction between the hydrophobic segments precedes the liquid–liquid phase separation. The addition of SDS to solutions of the gelling EHEC significantly changed the features of the DSC peaks, which indicates that SDS changes the association behavior of the polymer as the clouding temperature is approached. At certain compositions the phase separation is arrested and instead a gel forms.

## Introduction

Some ethyl(hydroxyethyl)celluloses (EHEC) of a rather hydrophobic type (*e.g.*, with cloud points (CP) of 30–35 °C in 1 wt % aqueous solutions) are known to give thermoreversible gels in the presence of ionic surfactants.<sup>1,2</sup> This means that a liquid solution can be converted to a transparent gel upon heating to temperatures slightly below its actual CP. The behavior is fully reversible as the gel liquefies upon cooling. The transition may occur at a temperature corresponding to that of the human/mammalian body, making the system interesting from a drug delivery point of view.<sup>3–7</sup>

Other, more hydrophilic EHEC, with higher CP's and a different relative degree of substitution of ethylene oxide (EO)-to-ethyl groups on the cellulose backbone, do not exhibit this behavior, although the viscosity can increase substantially upon addition of surfactant. Dilute and semidilute solutions of EHEC, both gelling and nongelling, have been studied by various techniques to gain information about the role of surfactant in the thermal gelation and to characterize the gels formed. For instance, the binding of surfactants to EHEC has been studied by ion-selective electrode<sup>8–10</sup> and self-diffusion measurements<sup>11,12</sup> and by titration microcalorimetry.<sup>9,13</sup> Surfactant aggregation number and ionization degree have been determined,<sup>12</sup> the viscosity has been measured,<sup>14</sup> and the rheological properties of the gels have been characterized.<sup>2,15,16</sup> Recently, a small-angle neutron scattering study of the structure of a thermosetting gel was carried out.<sup>17</sup> The aim of this work has been to combine the technique of high-sensitivity differential scanning calorimetry (HSDSC) with phase studies to gain insight into the thermal

events related to gelation, clouding, and phase separation in such systems. The phase behavior of two different gelling EHEC samples in 0.5 and 1.0 wt % solution containing varying amounts of SDS has been characterized between 20 and 80 °C. Using HSDSC we have studied thermal properties of different types of EHEC (both gelling and nongelling) in aqueous solution and investigated the effects of varying polymer and surfactant (SDS) concentrations. The influence of a nonionic surfactant (C<sub>12</sub>EO<sub>8</sub>) has also been studied.

Well-defined endothermic peaks were seen in DSC traces of samples of the three more hydrophobic EHEC in pure water at about the clouding temperatures (CP) of the solutions. The DSC trace for the more hydrophilic nongelling EHEC, with a CP at 65 °C, showed a different pattern as no peak could be detected. The size and shape of the DSC peaks were seen to vary somewhat between the more hydrophobic EHEC samples. This was also reflected in the macroscopic phase behavior in that the extension of the thermogelling regions with respect to polymer and surfactant concentrations was seen to differ.

We consider the transition peaks in the DSC traces to reflect that association of the polymer through interaction between the hydrophobic segments precedes liquid–liquid phase separation in solutions of the more hydrophobic EHEC. The addition of SDS modifies this association process as indicated by changes in the DSC traces. The peaks became broader and decreased in size with increasing surfactant concentration, particularly at compositions in the gelling region. We suggest that the thermal gelation of EHEC–SDS solutions can be described as an arrested phase separation. As the temperature is increased, a network develops with cross-links consisting of clusters of associated hydrophobic groups (or segments) from more than one polymer chain and a limited number of SDS molecules. Electrostatic repulsion between the clusters will stabilize the structure. These findings are consistent with

\* Corresponding author. Fax: ++46 46 2224533.

<sup>†</sup> Division of Thermochemistry.

<sup>‡</sup> Division of Food Technology.

<sup>®</sup> Abstract published in *Advance ACS Abstracts*, December 15, 1996.

**Table 1. Parameters of Investigated EHEC According to the Manufacturer**

batch name	notation	DS <sub>ethyl</sub>	MS <sub>EO</sub>	CP <sup>a</sup> (°C)	M <sub>n</sub>
CST 103	EHEC A	1.5	0.7	35	100 000
DVT 89017	EHEC B	1.9	1.3	34	100 000
DVT 88001	EHEC C	1.7	1.0	30	100 000
EHM 0	EHEC D	0.6–0.7	1.8	65	100 000

<sup>a</sup> CP values refer to 1.0% aqueous solutions.

results from a recent small-angle neutron scattering (SANS) study on a similar EHEC system, in which the gelation was ascribed to microphase separation.<sup>17</sup>

## Experimental Section

**Materials and Sample Preparation.** Three different samples of the same type of EHEC and another more hydrophilic batch were obtained from Akzo Nobel Surface Chemistry AB (Stenungsund, Sweden). Characteristic data for the samples are listed in Table 1. The values of DS<sub>ethyl</sub> and MS<sub>EO</sub> are the average number of ethyl and ethylene oxide groups, respectively, per anhydroglucose unit; CP denotes the cloud point in 1.00 wt % solution and M<sub>n</sub> the number-average molar mass. In the following, the samples are denoted EHEC A, EHEC B, EHEC C, and EHEC D. Dilute solutions were desalted and purified against Milli-Q water by an Ultrasette (Filtron) tangential flow device with a pore size of 10 kDa. The polymers were freeze-dried after dialysis. Sodium dodecyl sulfate SDS (BDH, 99%), C<sub>12</sub>EO<sub>6</sub>, and C<sub>12</sub>EO<sub>8</sub> (Nikko, Japan) were used as received.

The molar mass per monomer unit was calculated according to

$$M_m = 162.1 + 28.0\text{DS}_{\text{ethyl}} + 44.1\text{MS}_{\text{EO}}$$

where the first term is the molar mass of unreacted anhydroglucose.<sup>18</sup> Stock solutions of EHEC were prepared at least 5 days before sample preparation and stored in a refrigerator. EHEC–SDS solutions were equilibrated for 2 days to avoid any time-dependent effects as reported by Nilsson *et al.*<sup>19</sup> Only freshly prepared solutions were used.

**Phase Studies.** Solid surfactant and EHEC solution were weighed into glass tubes, sealed with Teflon-coated screw caps, and thoroughly mixed with a Whirlimixer shaking machine. The equilibration time was at least 48 h. Phase maps were determined in the temperature range 20–80 °C. The samples were equilibrated in a block thermostat (Grant BT3) for 1 h at each temperature and with an increase of about 5 °C per step. The transition regions were studied in more detail. The uncertainty in the transition temperatures is estimated to  $\pm 1$  °C. At least triplicates of samples of each composition have been studied with respect to phase and gelling behavior. The phase behavior was studied by visual observation, and the macroscopic fluidity was estimated to define regions with the thermogelling property. This very simple manual way to detect and locate gelation gave results in good agreement with those from more sophisticated methods, *i.e.*, rheological oscillatory<sup>2</sup> and steady-flow viscosity measurements.<sup>20</sup> We have chosen to use the notation *phase map* since the maps presented in this work differ from ordinary phase diagrams in the sense that we have locked the composition of the polymer and investigated the effects of the addition of SDS to the polymer solution. No tie lines, indicating the composition in phase-separated samples, are reported.

**Scanning Calorimetry.** Temperature scanning calorimetric measurements were made using a MicroCal MC-2 high-sensitivity differential scanning calorimeter (MicroCal, Northampton, MA). It is a differential instrument using twin, 1.2 mL total-fill cells. The Origin (Version 2.9) Software for DSC Data Collection and Analysis supplied by the manufacturer was used for instrument control, data acquisition, and analysis. The sample cell was filled with EHEC solution and the reference cell with the same amount of water. Samples and water were degassed and transferred to the cells with a syringe. The instrument measures the power required to keep

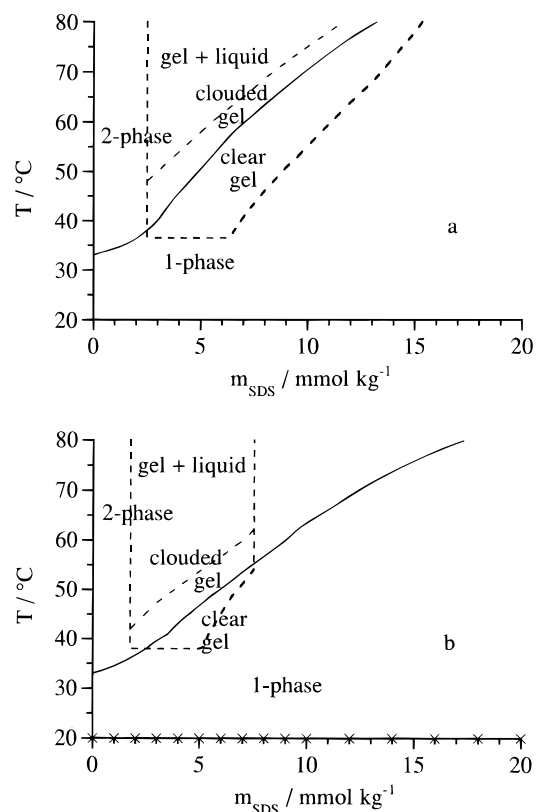


**Figure 1.** Phase maps of aqueous solutions of 1% EHEC A (a) and 1% EHEC B (b) with SDS. Crosses on the abscissa axis show SDS concentrations of samples studied. The solid line represents the cloud point curve and the broken lines indicate regions of high viscosity.

the temperature of the sample and reference cell equal while the temperature is raised at a constant rate. The results recorded in this way are called the sample traces. The reference trace is recorded under the same conditions with water filled in both cells. The excess heat capacity  $C_{p,\text{ex}}$  of the sample solution is calculated as a function of temperature from the difference between the sample and the reference traces. The enthalpy change for the transition  $\Delta H_{\text{cal}}$  was calculated from the area under the peak. The Progress Baseline option, which takes into account the heat capacity change accompanying the transition, was used to determine the baseline. The curves in Figures 4 and 5 do not show the lowering of  $C_{p,\text{ex}}$  accompanying the transition as baselines derived in this way have been subtracted from the original  $C_{p,\text{ex}}$  versus  $T$  curves. The enthalpy changes  $\Delta H_{\text{cal}}$  and heat capacities  $C_{p,\text{ex}}$  are expressed per mole of anhydroglucose unit, *i.e.*, repeat unit of the polymer. DSC calibration was achieved by supplying an electrical heat calibration pulse to the reference cell by a built-in heater and temperature calibration by using MicroCal's temperature standards. We have measured several of the systems with varying scanning rates and found that the peak shape and the temperature are independent of scanning rate over a range from 0.25 to 1.5 °C min<sup>-1</sup>. Transition kinetics are thus unimportant on the time scale of our experiments. Most of the systems were up-scanned from low to high temperature. For comparison, some of the systems were down-scanned.

## Results

**Phase Behavior.** Phase maps of 1% polymer solutions with SDS for the two hydrophobic EHEC samples that have CP's about 35 °C, called EHEC A (a) and EHEC B (b), are shown in Figure 1. A filled line represents the *turbidity boundary* (cloud-point curve), below which all samples are clear and consist of only one phase. Above this line the samples either scatter

(visible) light or are macroscopically phase separated. The broken lines indicate the domain where the most pronounced enhancement of viscosity is found. This area can further be divided into different parts depending on the visual appearance of the samples: *clear gels* formed below the turbidity line, *clouded gels*, which are not macroscopically phase separated but scatter light, and *gel + liquid*, where the gel coexists with a water-rich phase. The relative volume of the gel phase is here seen to decrease with increasing temperature (syneresis). The clear gels found below the turbidity boundary are considered thermodynamically stable. This assumption is based on equilibration tests, when the gels were kept for several weeks without any detectable changes. Moreover, the samples were seen to display a complete reversibility in the phase behavior; *i.e.*, clear gels that were slightly heated to form clouded gels could be reconstructed by lowering the temperature to the initial value. Such a "cycling" test could be repeated numerous times without any observable changes.

The general features of the two systems are the same, but the slope of the turbidity boundary with increasing SDS concentration is somewhat steeper for the EHEC A sample, and the gelation interval with respect to surfactant concentration is substantially wider than with EHEC B. There is a close relation between the slope/shape of the gelation domain and the turbidity boundary. The gelation is always seen to occur in the vicinity of the turbidity boundary. The lower gel boundary (gel point) for the EHEC A sample appears at a rather constant temperature with SDS concentrations between 2.5 and 6 mmol kg<sup>-1</sup>. It becomes more or less parallel to the turbidity boundary at higher surfactant concentrations (within the temperature range investigated). The gel point is also constant at lower surfactant concentrations (1.5–5 mmol kg<sup>-1</sup>) for the EHEC B sample. It is then shifted to higher temperatures with an increase/slope that is higher than the slope for the turbidity boundary, leading to a narrowing of the interval with clear gels. The temperature where the first signs of syneresis could be detected (which is indicated by the broken line separating the *clouded gel* from the *gel + liquid* area) seems to appear at a rather fixed distance from the turbidity boundary for both of the EHEC samples. Figure 2 shows the corresponding phase maps with a polymer concentration of 0.5%. No gelation is seen with EHEC B at this lower polymer concentration, and with EHEC A the gel domain is much smaller and restricted to a very narrow surfactant interval. It should also be noted that with the same surfactant concentrations, gelation occurs at higher temperatures compared to the 1% system. The slopes for the turbidity boundary appear to be steeper compared to the 1% polymer case. This difference can partly be accounted for when considering the difference in surfactant to polymer ratio, which is twice as high in Figure 2.

**Scanning Calorimetry. EHEC in Pure Water.** DSC curves for the four EHEC samples in this study are shown in Figure 3, where the apparent excess heat capacity  $C_{p,ex}$  for 1.00 wt % aqueous solutions are plotted as functions of temperature. The three more hydrophobic samples give well-defined peaks in the same temperature region. The peaks for the EHEC B and C samples are fairly sharp with a steep leading edge while the EHEC A sample gives a broader and lower peak. Table 2 summarizes DSC measurements on solutions containing between 0.25 to 2.50 wt % polymer. The

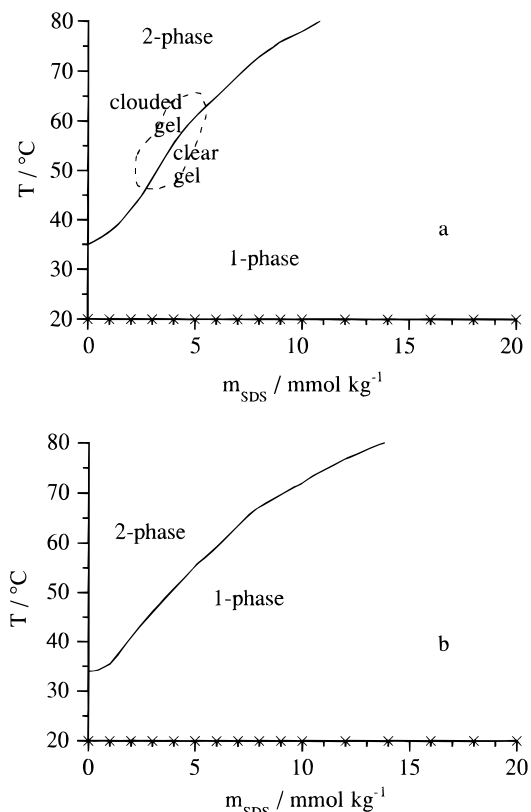


**Figure 2.** Phase maps of aqueous solutions of 0.5% EHEC A (a) and 0.5% EHEC B (b) with SDS. The solid line represents the cloud point curve. Sample composition is indicated by the crosses on the abscissa axis.

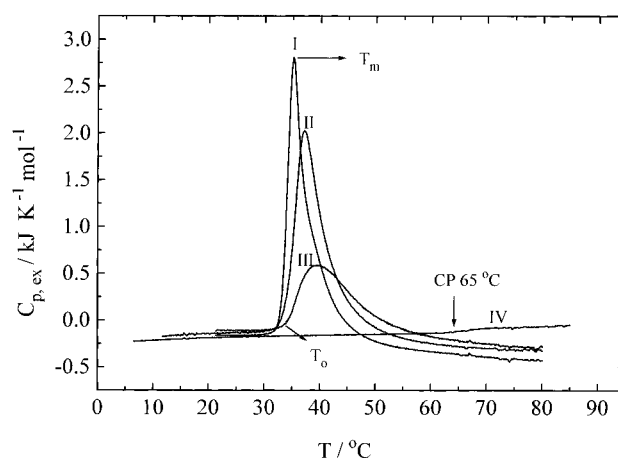


**Figure 3.** DSC traces of 1.00 wt % (I) EHEC C (CP 30 °C), (II) EHEC B (CP 34 °C), (III) EHEC A (CP 35 °C), and (IV) 2.00 wt % EHEC D (CP 65 °C) in water. In this and the following figures,  $C_{p,ex}$  is expressed per mole of anhydroglucose unit.

temperature of the peak maximum is denoted  $T_m$ ,  $T_0$  indicates the onset temperature, and  $\Delta T_{1/2}$  is the half peak width;  $\Delta H_{cal}$  is the enthalpy change calculated from the area under the peaks and  $\Delta C_{p,ex}$  is the difference between the extrapolated pre- and post-transition  $C_{p,ex}$ . It is worth noting that the hydrophobic EHEC samples have lower  $C_{p,ex}$  after the transition. When the EHEC content decreased, the onset temperature  $T_0$  shifted somewhat to higher temperature but the other characteristics of the peaks on the whole remained unchanged. Reported values for CP, the clouding temperature, fall between  $T_0$  and  $T_m$ . Thus the peaks in the DSC curves seem to reflect the liquid–liquid phase separation in the samples. The more

**Table 2. Characteristic Parameters for the Transition Peaks of EHEC in Aqueous Solution Derived from DSC Traces**

sample (wt %)	$T_0$ (°C)	$T_m^a$ (°C)	$\Delta T_{1/2}$ (°C)	$\Delta H_{cal}^{b,c}$ (kJ mol <sup>-1</sup> )	$\Delta C_p^b$ (J K <sup>-1</sup> mol <sup>-1</sup> )
EHEC A					
2.50	32.5	39.3	11.3	8.7	-78
1.00	32.7	39.7	10.9	8.7	-74
0.50	33.2	38.9	9.8	8.2	-35
0.25	33.9	39.6	9.5	8.3	-54
EHEC B					
2.00	32.4	37.1	5.5	15.2	-170
1.00	34.1	38.4	4.9	16.8	-200
0.75	34.5	38.5	5.4	16.7	-200
0.25	35.4	38.6	4.9	17.4	-150
EHEC C					
1.00	32.5	35.2	3.6	16.7	-240
0.25	31.5	34.6	5.7	18.8	-250

<sup>a</sup> Estimated uncertainty  $\pm 0.1$  °C. <sup>b</sup> Expressed per mole of anhydroglucose unit. <sup>c</sup> Estimated uncertainty  $\pm 0.5$  kJ mol<sup>-1</sup>.

**Table 3. Characteristic Parameters for the Transition Peaks of EHEC in Surfactant Solutions Derived from DSC Traces**

sample (wt %)	surfactant (mmol kg <sup>-1</sup> )	$T_0$ (°C)	$T_m$ (°C)	$\Delta T_{1/2}$ (°C)	$\Delta H_{cal}^a$ (kJ mol <sup>-1</sup> )	$\Delta C_p^a$ (J K <sup>-1</sup> mol <sup>-1</sup> )
EHEC A	SDS					
1.00	0	32.7	39.7	10.9	8.7	-70
	0.50	30.7	39.8	13.3	8.9	-140
	1.00	27.1	39.5	13.7	6.9	-150
	2.00	27.1	39.7	14.0	6.4	-310
	4.00	28.0	42.4	20.0	5.1	-300
	5.00	28.0	46.0	17.0	2.4	
	6.00	30.0	54	12.0	1.2	
	8.00	39	60	<i>b</i>	<i>b</i>	
	10.0	44	$\geq 70$	<i>b</i>	<i>b</i>	
0.5	0	33.2	38.9	9.8	8.2	-35
	4.00	39	52	15	2.8	
	6.00	45	64	20	4.9	
	8.00	52	71	<i>b</i>	$\geq 5^b$	
EHEC B	SDS					
1.00	0	33.1	37.0	5.7	16.7	-200
	0.50	30.3	37.0	8.2	16.0	-220
	1.00	30.0	37.0	9.5	15.5	-350
	4.00	28	39	14	7	-530
	6.00	38	49	25	4	
	8.00	44	58	$\geq 29^b$	$\geq 6^b$	
	10.0	52	<i>b</i>	<i>b</i>	<i>b</i>	
EHEC C	SDS					
1.00	0	32.5	35.2	3.6	16.7	-240
	4.00	26.4	36.5	12.8	4.5	-370
EHEC A	C <sub>12</sub> EO <sub>8</sub>					
1.00	4.00	29.1	39.0	12.1	8.1	-30
EHEC B						
1.00	4.00	30.0	36.8	8.2	16.2	-210

<sup>a</sup> Expressed per mole of anhydroglucose unit. <sup>b</sup> The end of the peak is beyond the temperature range of the experiment.

hydrophilic EHEC D sample showed a different behavior around the clouding temperature; see Figure 3. There is no peak and  $C_{p,ex}$  continues to increase above CP. Thus, only the more hydrophobic EHEC samples give well-defined peaks in the DSC curves. The endothermic  $\Delta H_{cal}$  and the decrease in  $C_{p,ex}$  probably arise from the aggregation and the accompanying dehydration of hydrophobic segments on the polymer chains. The  $\Delta H_{cal}$  and  $\Delta C_{p,ex}$  are significantly smaller for EHEC A than for the other two hydrophobic samples and the transition peak is broader.

**EHEC in SDS Solution.** DSC results of 1.00 wt % EHEC A in 0, 0.5, 2, and 4 mmol kg<sup>-1</sup> SDS are shown in Figure 4a. There is a smooth change in the DSC curves with increasing SDS concentration which spans the gel region; cf. Figure 1a. Characteristic parameters

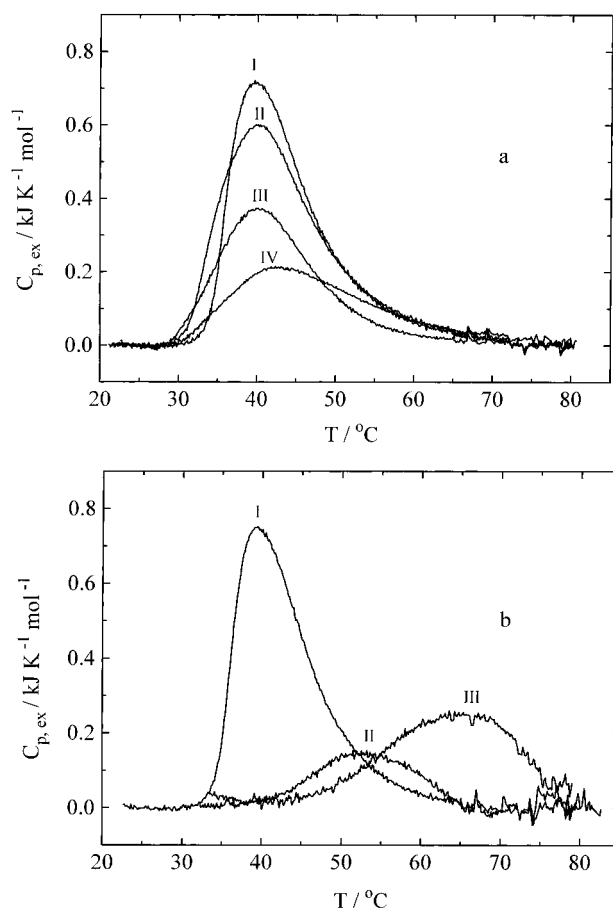


**Figure 4.** (a) DSC traces of 1.00 wt % EHEC A in (I) 0, (II) 0.5, (III) 2, and (IV) 4 mmol kg<sup>-1</sup> SDS. (b) DSC traces of 0.50 wt % EHEC A in (I) 0, (II) 4, and (III) 6 mmol kg<sup>-1</sup> SDS. (Baseline subtracted.)

of the peaks are summarized in Table 3, which also includes values for higher SDS concentrations for which the DSC traces are not shown. As the SDS concentration increased, the peaks became flatter and moved to higher temperatures. In 8 and 10 mmol kg<sup>-1</sup> SDS, the peaks extended beyond the range of the measurements. DSC traces of 0.50 wt % EHEC A with 0, 4, and 6 mmol kg<sup>-1</sup> SDS are shown in Figure 4b. The peak moved to higher temperatures upon addition of SDS;  $\Delta H_{cal}$  was lowered in 4 mmol kg<sup>-1</sup> SDS but increased in size in 6 mmol kg<sup>-1</sup> SDS which is above the gel region; cf. Figure 2a.

DSC traces of 1.00% EHEC B in 4, 6, and 8 mmol kg<sup>-1</sup> SDS solutions are shown in Figure 5. The solution with the highest SDS concentration is outside the gel-forming region and as with 0.5% EHEC A, the transition peak has become larger than the peak inside the region. The DSC results of 1.00 wt % EHEC B in SDS solutions of varying concentrations are summarized in Table 3. As seen from Figures 4 and 5, the addition of SDS to EHEC solutions significantly changed the features of the DSC traces. Already in 0.5 mmol kg<sup>-1</sup> SDS,  $T_0$  was shifted to lower temperature while  $T_m$  was unchanged. The peak became broader but  $\Delta H_{cal}$  stayed the same. In 1 and 2 mmol kg<sup>-1</sup> SDS,  $T_0$  was further lowered, but  $T_m$  remained unchanged while  $\Delta H_{cal}$  decreased. In 4 mmol kg<sup>-1</sup> SDS, which is the optimum SDS concentration for gel formation in these EHEC systems,  $T_0$  still was lower than in pure water,  $T_m$  was shifted to higher temperature and  $\Delta H_{cal}$  was much reduced; cf. Table 3. As the SDS concentration further increased,  $T_0$  and  $T_m$  changed to higher temperatures, the peaks further

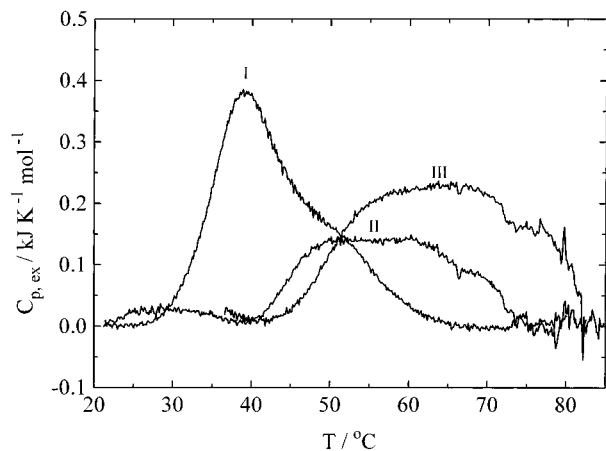


**Figure 5.** DSC traces of 1.00 wt % EHEC B in (I) 4, (II) 6, and (III) 8 mmol kg<sup>-1</sup> SDS. (Baseline subtracted.)

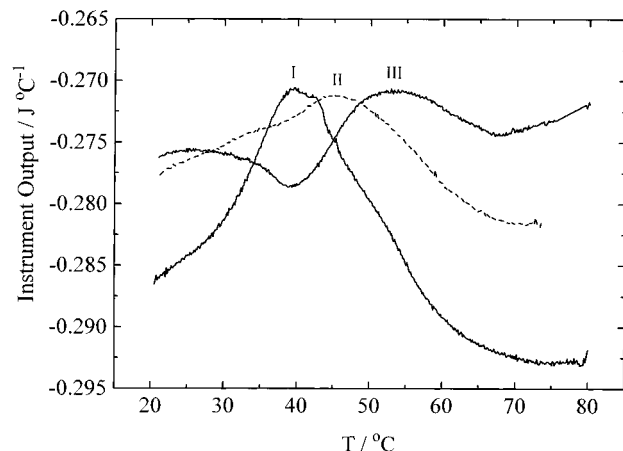


**Figure 6.** Instrument output of DSC traces of (I) 1.00, (II) 0.75, and (III) 0.50 wt % EHEC B in 4 mmol kg<sup>-1</sup> SDS.

broadened, and  $\Delta H_{cal}$  continued to decrease as long as it was in the gel region. At SDS concentration above the gelling range, the peaks started to increase in size and became less broad.

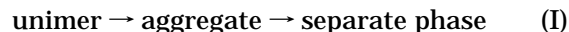
**EHEC Content Dependence.** DSC traces of 0.50, 0.75, and 1.00 wt % EHEC B in 4 mmol kg<sup>-1</sup> SDS are shown in Figure 6. These are uncorrected curves where the ordinate axis gives the instrument output expressed as the difference in heat capacity between sample and reference cells. The sample containing 1.00 wt % polymer gives a clear gel when heated above 38 °C which upon further warming becomes cloudy above 43 °C; see Figure 1b. The 0.50 wt % solution does not gel but has a cloud point at 52 °C. (The phase behavior of the 0.75 wt % solution is not known.) As seen, the shape of the curves varied significantly with EHEC content. The 1% solution showed a pronounced peak with maximum at the clouding temperature. Already from the start of the scan, the heat capacity of the solution changed significantly with increasing temperature, as seen from the fairly steep slope of the initial part of the curve. This indicates that in the presence of SDS, polymer association starts already at room temperature. In the 0.75% solution the transition peak was flatter and broader without any defined onset and with a maximum at a slightly higher temperature than in the 1.00% solution. The curve in 0.50% solution looks different with a decreasing heat capacity from about 25 to 40 °C and then increasing heat capacity to give a well-defined peak centered at about CP. It can be noted that the heat capacity of the 1.00% solution was significantly

lower after the transition peak while it was higher in the 0.50% solution. The difference between the change of the heat capacity with temperature for the 1.00 and 0.50% solutions in the beginning of the scans indicates significant differences in the interaction of SDS with EHEC at gelling and nongelling concentrations.

**EHEC in C<sub>12</sub>EO<sub>8</sub> Solution.** The DSC traces of 1.00 wt % solution of EHEC A and EHEC B in 4 mmol kg<sup>-1</sup> C<sub>12</sub>EO<sub>8</sub> looked about the same as those in pure water. Only  $T_0$  was lowered a few degrees (see Table 3), which agreed with the observed lowering of the cloud point of the solutions (by visual inspection). C<sub>12</sub>EO<sub>8</sub> has a cmc of  $9 \times 10^{-5}$  mol kg<sup>-1</sup> at 25 °C in water so in 4 mmol kg<sup>-1</sup> solution it will predominantly be in the form of micelles. Zhang *et al.*<sup>21</sup> concluded from results of NMR self-diffusion measurements on the EHEC A–C<sub>12</sub>EO<sub>8</sub> system that there is an attractive interaction between C<sub>12</sub>EO<sub>8</sub> micelles and the polymer.

## Discussion

**Nongelling Polymer–Water Systems.** Aqueous solutions of EHEC in water show liquid–liquid phase separation as the temperature is increased. The phase separation or clouding temperature (CP) varies with the nature of the substituents and the degree of substitution. Schild and Tirrell<sup>22</sup> noted that the endothermic transition peaks observed in DSC studies of aqueous polymer solutions showing liquid–liquid separation coincided with the increase in solution turbidity, which is typically associated with the onset of phase separation. In a recent paper, Armstrong *et al.*<sup>23</sup> discussed two schemes for the phase separation of solutions of poly(propylene oxide) (PPO) in water. According to one scheme, polymer chains associate to form aggregates below the clouding temperature and then interact as the temperature is increased to form a separate polymer-rich phase. Alternatively, the polymer exists as unimers (single polymer molecules) up to the phase separation temperature. Using the mass action law model and the van't Hoff equation, they simulated the DSC output assuming an aggregation process. The calculated and experimental DSC curves showed very good agreement, which indicates that in this type of system, aggregation may precede phase separation upon heating. Applying the same reasoning as Armstrong *et al.*,<sup>23</sup> we propose that the liquid–liquid phase separation in EHEC–water solutions can occur in two possible ways:



Aqueous solutions of the three more hydrophobic EHEC samples in our study exhibited well-defined endothermic peaks at temperatures around their CP's (about 30–35 °C), whereas no peak could be detected for the more hydrophilic sample (CP at 65 °C); see Figure 3. We think that the striking difference between the thermograms of the gelling and nongelling EHEC indicates a difference in the polymer–polymer association pattern. The endothermic peaks may reflect polymer association by means of hydrophobic interaction (and dehydration) of the hydrophobic groups. In the concentration range studied, both inter- and intramolecular associations are likely to occur. Recent results from a small-angle neutron scattering study of *inter alia* semidilute EHEC B in D<sub>2</sub>O solution indicate that the polymer could be weakly associated (or incompletely dissociated) already at 20 °C, *i.e.*, well below the CP (at 34 °C).<sup>17</sup> An

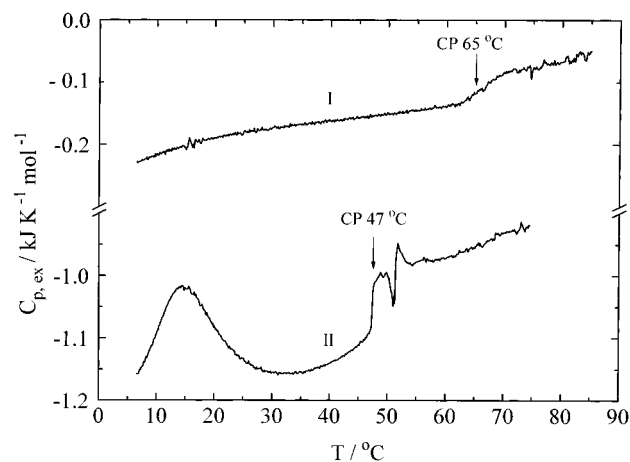


**Figure 7.** DSC traces of (I) 2.00 wt % EHEC D and (II) 5.00 wt %  $C_{12}EO_6$  in water.  $C_{p,ex}$  of EHEC D is calculated per mole of anhydroglucose unit and  $C_{12}EO_6$  per mole of monomer.

enlargement of the DSC trace of the more hydrophilic EHEC D sample showed a characteristic step in the apparent  $C_p$  at the clouding temperature similar to that observed by Armstrong *et al.*<sup>23</sup> for PEO (in salt solution?); see Figure 7. The DSC trace for a 5 wt % solution of the nonionic surfactant  $C_{12}E_6$  is also included in Figure 7. The cloud point of the  $C_{12}EO_6$  solution is about 47 °C,<sup>24,25</sup> which coincides with the step to higher  $C_{p,ex}$  in the DSC curve. (The broad peak centered at 15 °C for  $C_{12}EO_6$  may stem from micellar growth.<sup>26,27</sup>) Thus, liquid–liquid phase separation in PEO, EHEC D, and  $C_{12}EO_6$  solutions gives similar changes in  $C_{p,ex}$ . The features of the DSC curve for EHEC D indicate that in this system, phase separation takes place without preceding aggregation. The more hydrophobic EHEC is substituted with about twice the number of ethyl groups per anhydroglucose unit. Thus, depending on the extent of hydrophobic substitution, liquid–liquid phase separation can take place according to either of the suggested paths.

The variation of the size and the shape of the endothermic peaks for the three more hydrophobic EHEC samples in water, illustrated in Figure 3, could be due to different degrees of heterogeneity in the substitution along the polymer chain. The batch called EHEC A has a significantly smaller and broader peak than the other two samples and we think that these features might be due to a more blocky structure with a more extended association of hydrophobic groups well below CP. The significantly lower  $\Delta C_p$  for the EHEC A sample supports this assumption; see Table 2. The change in  $\Delta C_p$ , which is the difference between the apparent heat capacity of EHEC before and after clouding, probably arises from changes in hydrophobic hydration accompanying association of alkyl groups. Large negative heat capacity changes arising from the dehydration of hydrophobic groups characterize, for instance, micelle formation of amphiphiles in aqueous solution.

**Gelling Systems.** Normally, aqueous solutions of EHEC do not form gels. The more hydrophobic EHEC we have used may form thermoreversible gels after addition of ionic surfactants. Conditions for gel formation in the EHEC–SDS systems are shown in Figures 1 and 2. As seen, there are restrictions for gelation with respect to both surfactant and polymer concentration. There is a well-defined lower surfactant concentration limit of about 2 mmol kg<sup>-1</sup> while the upper limit varies

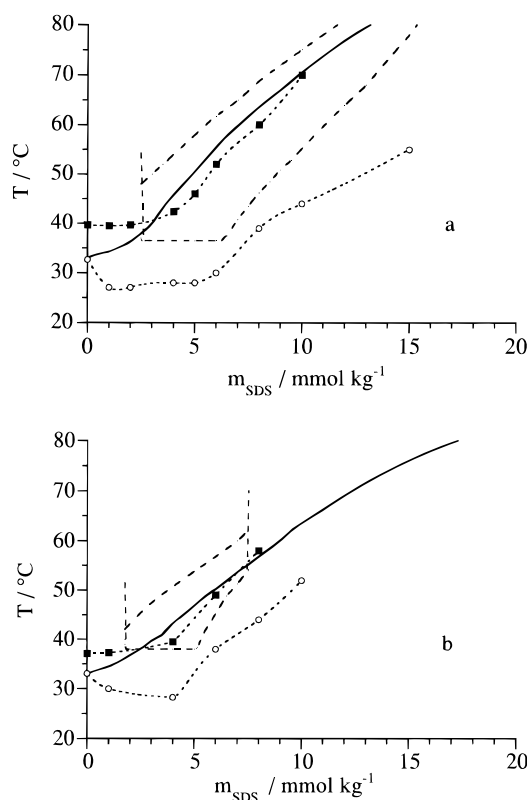


**Figure 8.** Phase maps and DSC results of (a) 1.00 wt % EHEC A and (b) 1.00 wt % EHEC B in different concentrations of SDS: (---) boundary of gel region; (—) cloud point line; (○) onset temperature  $T_0$  of DSC peaks; (●) peak maxima  $T_m$ .

between different EHEC samples. Addition of SDS will increase the viscosity of moderately dilute and semi-dilute EHEC solutions. At ambient temperatures, the viscosity goes through a maximum in solutions containing between 4 and 6 mmol kg<sup>-1</sup> of SDS, depending on the EHEC content. Depending on the SDS concentration, temperature changes will affect the properties of EHEC–SDS solutions in different ways. At SDS concentrations up to about 2 mmol kg<sup>-1</sup>, the increase of the clouding temperature with increasing surfactant concentration is the main effect; *cf.* Figures 1 and 2. At SDS concentrations above 2 mmol kg<sup>-1</sup>, the viscosity will increase with increasing temperature and eventually a clear, stiff gel forms. This clear gel is apparently thermodynamically stable. As the temperature is further increased, the gel becomes turbid but still shows long-term stability. At still higher temperatures, macroscopic phase separation starts and the gel will expel water. From the work of Kamenka *et al.*<sup>12,28</sup> we know that the aggregation number of surfactant aggregates bound to EHEC decreases substantially with increasing temperature from 22 at 20 °C to 12 at 40 °C in 0.50 wt % EHEC B solution containing about 4 mmol kg<sup>-1</sup> SDS. The rearrangement of SDS from larger to smaller clusters increases the number of aggregates. This, in combination with the increased amount of hydrophobic domains created by the thermally induced association of polymer side chains, may be the cause of gelation. The phase maps are combined with results from the DSC measurements in Figure 8. In pure water the onset temperature of the peaks in the DSC curves,  $T_0$ , coincides with the CP where the polymer has aggregated to give domains large enough to scatter light. The maximum temperature  $T_m$  indicates the temperature for the highest apparent heat capacity of the system, that is where the polymer association increases the

most. When SDS is added,  $T_0$  decreases, which indicates that association starts at a lower temperature but the polymer aggregates grow more slowly in the presence of SDS and a gap develops between  $T_0$  and the clouding temperature. At low SDS concentrations  $T_m$  is unchanged but in the gel region it approaches the cloud point line. The sharp increase in viscosity causing the gelation is not detectably reflected in the DSC curves. The presence of SDS affects both the size and the shape of the transition peaks; see Figures 4–6. For instance, the transition enthalpies for the three hydrophobic EHEC in 1.00 wt % containing 4 mmol kg<sup>-1</sup> SDS are only one half to one third of the values in water; see Table 3. The decrease stems from changes in polymer–polymer interactions as the enthalpy contribution from SDS is too small to be of significance; the SDS concentration is only one tenth of the concentration of anhydroglucose units. Thus, SDS modifies the association of EHEC chains to allow gel formation instead of phase separation. However, SDS is effective only at low concentrations. Above an SDS concentration of 7.5 mmol kg<sup>-1</sup> in 1.00 wt % EHEC B, no gel is formed and the transition enthalpy starts to increase.

We can get some enlightenment from a recent study of a hydrophobically modified EHEC–SDS system.<sup>9</sup> The EHEC used was EHEC D (see Table 1) modified with 1.7 mol % nonylphenol and denoted HM–EHEC. Semidilute HM–EHEC forms hydrophobic microdomains of micellar type by the association of the nonylphenol groups. SDS ion-selective electrode work showed that pronounced, noncooperative binding of SDS to 1.00% HM–EHEC started below 0.1 mmol kg<sup>-1</sup> of SDS. The fluorescence measurements indicated that the aggregation number of SDS in the mixed micelles is low and that the number of hydrophobic microdomains is constant and independent of the surfactant concentration up to around 3 mmol kg<sup>-1</sup> SDS.<sup>9</sup> The viscosity enhancement observed for hydrophobically modified polymers upon addition of surfactant was considered to arise from an increased number of intermolecular aggregates at the expense of intramolecular ones, which would lead to an increased number of elastically active chains in the solution.<sup>29,30</sup> Both the SANS study<sup>17</sup> and our DSC results indicate that unmodified but more hydrophobic EHEC also self-associates, but to a lower extent than hydrophobically modified EHEC such as HM–EHEC. The lowering of the onset temperature  $T_0$  in the DSC experiments already in 0.5 mmol kg<sup>-1</sup> SDS (Figure 4) indicates that the surfactant starts to interact with 1.00 wt % EHEC at concentrations well below the concentration for cooperative binding. This premicellar polymer–SDS interaction was also observed in the self-diffusion measurements by Kamenka *et al.*<sup>12</sup> When SDS is added to an unmodified EHEC solution, it may initially bind to hydrophobic domains formed by the associated substituents.

A possible mechanism for the formation of thermoreversible gels in EHEC–SDS systems might be described as follows. At room temperature, semidilute EHEC solutions have the property of normal high molar mass polymer solutions. They appear a little viscous through polymer chain entanglement and some hydrophobic domains may be formed by the association of hydrophobic segments. Increasing temperature favors polymer–polymer association and large EHEC aggregates may form. Depending on the swelling and associating balance, the aggregates can either be microscopically phase separated or further associate to

separate into macroscopic polymer-rich and water-rich phases.

When SDS is added to an EHEC solution at ambient temperature, the SDS monomers will first bind to the existing hydrophobic microdomains. After saturating the microdomains, SDS will start to associate cooperatively to form mixed micelles involving substituents from one or more EHEC chains. Aggregation of SDS will tend to bring polymer chains together up to an added surfactant concentration of  $[\text{SDS}]_{\text{max}}$ , at which the optimum number of intermolecular cross-links have been formed.  $[\text{SDS}]_{\text{max}}$  will vary with EHEC content.<sup>6,31</sup> The viscosity maxima discussed above can be regarded as estimates of  $[\text{SDS}]_{\text{max}}$ . The aggregates are charged and electrostatic repulsion hinders too close contact between the polymer chains and an equilibrium state of association and repulsion is reached. The SDS molecules can be regarded as ion splints binding together the hydrophobic substituents to form clusters and at the same time stabilize the polymer network and prevent it from collapse by electrostatic repulsion. The formation of the thermoreversible gel can be described as an arrested phase separation. As the temperature is further increased, hydrophobic interaction between EHEC segments will dominate and the balance between connection and repulsion of the SDS-bound EHEC segments will be broken. The gel goes into syneresis.

At concentrations of added surfactant above  $[\text{SDS}]_{\text{max}}$ , additional surfactant aggregates are available for the “solubilization” of the polymer-bound hydrophobes. Consequently, the average number of bound hydrophobes per surfactant aggregate will decrease, thereby reducing the number of effective micellar-type cross-links and thus decreasing the viscosity of the system. When the temperature of the system increases, hydrophobic segments of EHEC still tend to associate but higher temperature is needed for the hydrophobic segments to associate and create enough junction points for a gel to form at higher SDS concentrations.

The number of hydrophobic microdomains available for enhanced binding of SDS and the associating ability of the segments may be different for the three hydrophobic EHEC samples we have used. An unequal distribution pattern of the substituents along the polymer chain for the EHEC A and EHEC B may be responsible for the differences in the gelling behavior. We believe that EHEC A has a more blocky distribution with hydrophobic segments separated by more hydrophilic ones. Such a polymer would more easily find configurations that would be satisfactory for both types of segments. The surfactants will bind at the hydrophobic parts and these segments will be connected by the more hydrophilic parts which stay hydrated. The balance between intra- and intermolecular association and its surfactant dependence will be affected by differences in the degree of blockiness.

In the small-angle neutron scattering (SANS) study of the structure of an EHEC–surfactant system by Cabane *et al.*,<sup>17</sup> it was found that the structure in the gelling region can be described as small lumps of polymer covered by a shell of surfactant. In pure EHEC solution of the same temperature and concentration, the polymer lumps were much larger (but still of finite size). Thus, the effect of surfactant is to fragment the domains of the polymer-rich phase into smaller lumps. Our model for the function of the surfactant in the formation of thermoreversible EHEC gels is consistent with these findings.

### Concluding Remarks

The pronounced endothermic peaks observed at about the clouding temperature in HSDSC traces of aqueous solutions of gelling EHEC are considered to indicate that polymer-polymer association through hydrophobic interaction between the substituents precedes liquid-liquid phase separation. No transition peak was observed for a solution of a nongelling EHEC, which gave only a small step in the excess heat capacity at the cloud point. Addition of SDS to solutions of gelling EHEC changed the shape and the size of the transition peaks. The changes were most pronounced at compositions in the gelling region.

SDS starts to interact with the more hydrophobic EHEC at concentrations well below the critical concentration for cooperative aggregation. This indicates that hydrophobic microdomains, analogous to those in solutions of hydrophobically modified polymers, may exist already at ambient temperatures. In semidilute solutions, the hydrophobic association increases as the temperature is increased and addition of SDS at low concentrations induces the formation of cross-links. At certain concentrations a polymer network develops and a gel is formed. The incorporation of an ionic surfactant stabilizes the network and prevents it from collapse. In dilute EHEC solution the interaction between SDS and EHEC has a different character as indicated by the difference between the change of the heat capacity with temperature for dilute and semidilute EHEC solutions containing SDS.

**Acknowledgment.** We wish to thank Ingegerd Lind for purifying the EHEC samples. Peter Sellers is thanked for performing initial experiments with K.L. This study has been supported by the Swedish National Board for Technical and Industrial Development (NUTEK).

### References and Notes

- (1) Carlsson, A.; Karlström, G.; Lindman, B. *Colloids Surf.* **1990**, *47*, 147.
- (2) Nyström, B.; Walderhaug, H.; Hansen, F. K. *Langmuir* **1995**, *11*, 750.
- (3) Lindman, B.; Carlsson, A.; Thalberg, K.; Bogentoft, C. *Actual. Chim.* **1991**, May-June, 181.
- (4) Pereswetoff-Morath, L. Ph.D. Thesis, Uppsala University, 1995.
- (5) Lindell, K.; Engström, S. *Int. J. Pharm.* **1993**, *95*, 219.
- (6) Holmberg, C. Ph.D. Thesis, Uppsala University, 1995.
- (7) Nilsson, S. Ph.D. Thesis, Uppsala University, 1995.
- (8) Carlsson, A.; Lindman, B.; Watanabe, T.; Shirahama, K. *Langmuir* **1989**, *5*, 1250.
- (9) Thuresson, K.; Söderman, O.; Hansson, P.; Wang, G. *J. Phys. Chem.* **1996**, *100*, 4909.
- (10) Bloor, D. M.; Wan-Yunus, W. M. Z.; Wan-Badhi, W. A.; Li, Y.; Holzwarth, J. F.; Wyn-Jones, E. *Langmuir* **1995**, *11*, 3395.
- (11) Walderhaug, H.; Nyström, B.; Hansen, F. K.; Lindman, B. *J. Phys. Chem.* **1995**, *99*, 4672.
- (12) Kamenka, N.; Burgaud, I.; Zana, R.; Lindman, B. *J. Phys. Chem.* **1994**, *98*, 6785.
- (13) Wang, G.; Olofsson, G. *J. Phys. Chem.* **1995**, *99*, 5588.
- (14) Holmberg, C.; Nilsson, S.; Singh, S. K.; Sundelöf, L.-O. *J. Phys. Chem.* **1992**, *96*, 871.
- (15) Nyström, B.; Lindman, B. *Macromolecules* **1995**, *28*, 967.
- (16) Nyström, B.; Kjøniksen, A.-L.; Lindman, B. *Langmuir*, in press.
- (17) Cabane, B.; Lindell, K.; Engström, S.; Lindman, B. *Macromolecules* **1996**, *29*, 3188.
- (18) Carlsson, A.; Lindman, B.; Nilsson, P.-G.; Karlsson, G. *Polymer* **1986**, *27*, 431.
- (19) Nilsson, S.; Holmberg, C.; Sundelöf, L.-O. *Colloid Polym. Sci.* **1994**, *272*, 338.
- (20) Lindell, K., unpublished results.
- (21) Zhang, K.; Jonströmer, M.; Lindman, B. *J. Phys. Chem.* **1994**, *98*, 2459.
- (22) Schild, H. G.; Tirrell, D. A. *J. Phys. Chem.* **1990**, *94*, 4352.
- (23) Armstrong, J.; Chowdhry, B.; O'Brien, R.; Beezer, A.; Mitchell, J.; Leharne, S. *J. Phys. Chem.* **1995**, *99*, 4590.
- (24) Clunie, J. S.; Goodman, J. F.; Symons, P. C. *Trans. Faraday Soc.* **1969**, *65*, 287.
- (25) Mitchell, D. J.; Tiddy, G. J. T.; Waring, L.; Bostock, T.; McDonald, M. P. *J. Chem. Soc., Faraday Trans. 1* **1983**, *79*, 975.
- (26) Brown, W.; Johnson, R.; Stilbs, P.; Lindman, B. *J. Phys. Chem.* **1983**, *87*, 4548.
- (27) Brown, W.; Rymdén, R. *J. Phys. Chem.* **1987**, *91*, 3565.
- (28) Zana, R.; Binana-Limbelé, W.; Kamenka, N.; Lindman, B. *J. Phys. Chem.* **1992**, *96*, 5461.
- (29) Annable, T.; Buscall, R.; Ettelaie, R.; Shepherd, P.; Whittlestone, P. *Langmuir* **1994**, *10*, 1060.
- (30) Semenov, A. N.; Joanny, J.-F.; Khokhlov, A. R. *Macromolecules* **1995**, *28*, 1066.
- (31) Piculell, L.; Thuresson, K.; Ericsson, O. *Faraday Discuss.* **1995**, 101.

MA960125H